ISSN (Print) : 0974-6846
Indian Journal of Science and Technology, *Vol 10(17), DOI: 10.17485/ijst/2017/v10i17/110380, May 2017* ISSN (Online) : 0974-5645

CO_2 Reforming of Methane over Ni/Ce-SBA-15: Effects of Ce Addition

Nurul Ainirazali*, Nurul Ainun Nabihah AbGhazab, Herma Dina Setiabudi and Chin Sim Yee

Faculty of Chemical and Natural Resources Engineering Universiti Malaysia Pahang, Lebuhraya Tun Razak, 26300 Gambang, Pahang, Malaysia; ainirazali@ump.edu.my

Abstract

Background/Objectives: The effects of Ce loading (1-7 wt%) on the properties of Ni/SBA-15 andCO_2 dry reforming with methane was studied. **Methods/StatisticalAnalysis:** The physicochemical properties of the catalysts were analyzed by XRD, BET, TEM and FTIR. Catalytic performance of catalyst was performed using a fixed bed reactor at 700°C. **Findings:** NCS7 catalyst had the highest activity and good stability with CH_4 conversion, CO_2 conversion and H_2/CO ratio of 94.9%, 95.1%, and 0.99, respectively. This can be attributed to the Ce ensuring a good Ni dispersion and inhibited the carbon deposition on the catalyst surfaces. Moreover, high Ce loading of NCS7 promoting the formation of a significant synergy effect between Ni active sites with SBA-15 for target reaction. **Application/Improvements:** The result presented is very promising to improve the GHGs conversion strategies for the production of useful chemical products.

Keywords: Cerium, Nickel, SBA-15, Sol-Gel, Syngas

* *Author for correspondence*

NCS1, NCS3, NCS5 and NCS7 for different Ce loading of 1, 3, 5 and 7 wt%, respectively.

2.2 Catalyst Characterization

The characteristics of the synthesized catalysts were investigated using XRD, BET, TEM and FTIR. The phase identification of catalyst was verified by X-ray diffraction (XRD) (Rigaku model MiniflexII, 30 kW) using a Cu Kα radiation (λ = 1.5405Å) in the range of 2θ = 10 – 80°. The measurement of multi-point BET surface area, pore diameter and pore volume for catalysts was conducted using AUTOSORB-1 model AS1 MP-LP instrument at 77 K. The structural morphologies of the catalysts were analyzed using a Philip CM12 transmission electron microscope operated at 80 kV. Fourier-Transform Infrared (FTIR) Spectroscopy analysis was carried out using Thermo Nicolet Avatar 370 DTGS model in KBr matrix in the range of 500 – 4000 cm^{-1} to verify the effect of Ce species toward the chemical bonding and interaction with the SBA-15

2.3 Catalyst Activity Test

The CO_2 reforming of methane was conducted in a fixed-bed reactor (1 cm ID and 43 cm in length) at 700°C and atmospheric pressure. 0.2 g of catalyst with average particle size of 100-140 µm was packed and placed vertically in a tubular furnace. Prior to the reaction, the catalyst was reduced in a H_2 flow of 50 ml/min for 3 h at 800°C. Then, a mixture of CH_4 and CO_2 was fed into the reactor at CH_4/CO_2 ratio of 1 with space time was about 20.26 s. The composition of gaseous effluent from the reactor outlet was analyzed with an Agilent 6890 Series Gas Chromatograph (GC) equipped with Thermal Conductivity Detectors (TCD).

3. Results and Discussion

3.1 Characterization of Catalyst

Figure 1 showed the XRD patterns of NCS catalyst loaded with different Ce loading. The characteristic of the amorphous SiO_2 wall of SBA-15 was indicated by a broad diffraction peak centered at 2θ ≈ 22.5° that decreased with increasing of Ce content.[8] This evidences that the presence of Ce was destroyed the ordered structure of SBA-15 due to the interaction of Ce with silica of SBA-15; these features are enhanced by increase of Ce content. The sharp diffraction peaks were observed at 37.3°, 43.3°, 44.5°, 51.8°, 63.0°, 75.4° and 76.4° attributed to Ni metal crystalline phases were indicated in all samples.[7,9] However, the intensities decreased with the increasing of Ce loading, indicating the Ni species are well dispersed with the higher Ce content. The characteristic peaks of CeO_2 at 28.6°, 33.1°, 47.5° and 56.3°, can be clearly observed in XRD spectra of all catalysts, except for the NCS1 catalyst, in which the diffraction peaks can be attributed to (1 1 1), (2 0 0), (2 2 0) and (3 1 1) planes of cubic CeO_2 with fluorite structure (Fm3m, JCPDS: 43–1002).[10] The peaks were more intense with the increasing of Ce loading from 3-7 wt%, corresponding to a more crystallite CeO_2 phase deposited outside the SBA-15 support. When 1 wt% of Ce was loaded onto SBA-15, no CeO_2 characteristic peaks were observed due to the complete incorporation of Ce species into the SBA-15 framework.

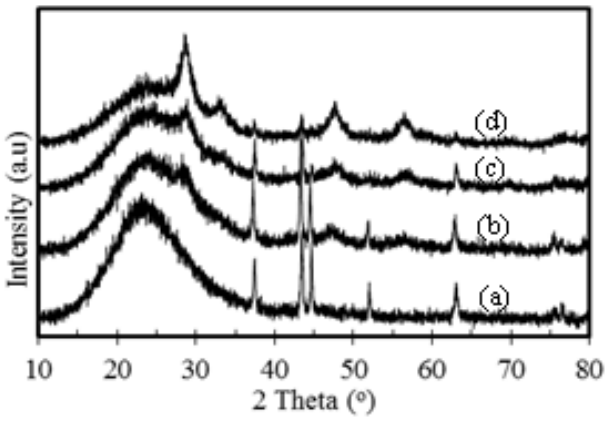

Figure 1. XRD patterns of (a) NCS1, (b) NCS3, (c) NCS5 and (d) NCS7.

The textural parameters of NCS catalysts obtained from the N_2 adsorption isotherms are shown in Table 1. The surface area and total pore volume of NCS catalysts were gradually decreased from 670.69 to 571.39 m^2g^{-1} and 155.71 to 108.30 cm^3g^{-1}, respectively after introducing of Ce from 1 to 7 wt%. These results indicating that the SBA-15 pores are filled by dispersing CeO_2 and the SBA-15 structure was destroyed during the incorporation of Ce and Ni. The decreased in the surface area with the increasing of Ce content has been observed in metal-modified SBA-15.[9-11] In contrast, the average pore diameter

of the NCS increased as the Ce loading increased from 1 to 7 wt%, indicating the expansion of the SBA-15 pores. This result could be attributed to the incorporation of Ce (0.87Å) with the SBA-15, which has bigger ionic radius than Si (0.41Å) leading to the larger unit cell of catalyst.[10]

Table 1. Textural properties of NCS catalysts

Catalyst	BET surface area (m^2 g^{-1})	Total pore volume (cm^3 g^{-1})	Average pore diameter (nm)
NCS1	670.69	155.71	3.73
NCS3	659.72	154.09	4.52
NCS5	643.06	147.74	5.28
NCS7	501.39	108.30	5.59

TEM image of NCS7 in Figure 2 presents the ordered meso-structure and hexagonal pore structure characteristic of SBA-15 with the lattice d-spacing of 8.3 nm. This result indicates that Ni and Ce incorporated on SBA-15 were successfully synthesized by sol-gel method. Moreover, the presence of some metal aggregates in the external surface of SBA-15 observed in TEM analyses of NCS7 is consistent with the XRD, which suggest the metal crystallite larger than the pore diameter and deposited outside of the SBA-15 support.

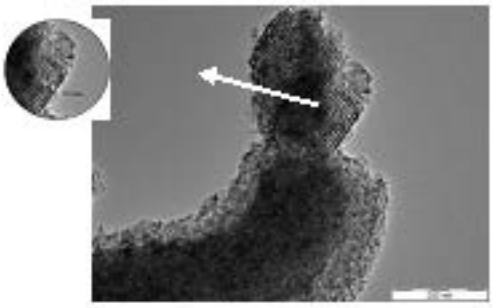

Figure 2. TEM image of the NCS7 catalyst.

Figure 3 presents the FTIR spectra of NCS1, NCS3, NCS5 and NCS7 in the range of 1400 – 500 cm^{-1} and 3700 – 2500 cm^{-1}. The band observed at 3420 cm^{-1} could be assigned to the stretching vibrations of the surface silanol groups and the adsorbed H_2O.[11] The symmetric stretching vibration (Si-O-Si)sym of tetrahedral SiO_4 structure and the anti-symmetric vibration non-bridging oxygen atoms (Si-Oδ-) of Si-O-H bonds are observed at 801 cm^{-1} and 1040 cm^{-1}, respectively.[12] According to Ma *et al*, Si-O-Si bands at 801 cm^{-1} and 1040 cm^{-1}were associated with the condensed silica network formation of SBA-15.[13]

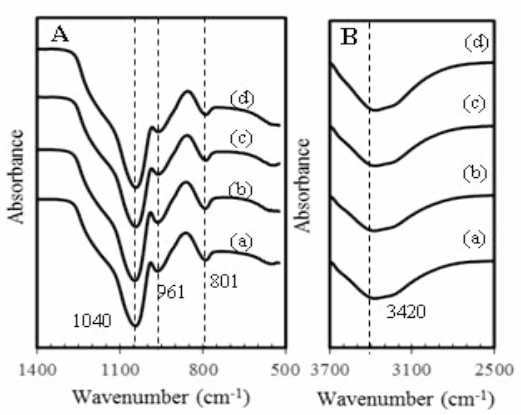

Figure 3. FTIR spectra of (a) NCS1; (b) NCS3; (c) NCS5 and (d) NCS7 catalysts in the range of (A) 1400 – 500 cm^{-1}; (B) 3700 – 2500 cm^{-1}.

The intensity of the bands at 1040 cm^{-1} and 3420 cm^{-1} is slightly decreased as the Ce loading increased reflecting to the Ce interaction with the anti-symmetric vibration nonbridging oxygen atoms (Si-Oδ-) of Si-O-H and substitution of O-H with O-Ce, respectively. The band at 961 cm^{-1} is indicative of the presence of SiO units bonding to the metal, evidenced the interaction of Ce with Si-Oδ- of SBA-15 by substitution of O-H with O-Ce.[14]

3.2 Catalytic Performance

The effect of Ce loading on CO_2 reforming of methane results over NCS are presented in Figure 4. The results revealed that when Ni loading was 5 wt%, the addition of Ce (1-7 wt%) on SBA-15 was able to enhance both the conversions of CO_2 and methane. Over all the catalysts, conversion of CO_2 was higher than CH_4 conversion and the H_2/CO ratio was less than one due the influence of Reverse Water-Gas Shift (RWGS) reaction during the testing. These fact phenomena were in good agreements with those reported for CO_2 reforming of methane.[7,15]

The highest catalytic performance was obtained by NCS7 with the CH_4 conversion, CO_2 conversion and H_2/CO ratio of 94.9%, 95.1%, and 0.99, respectively. This result suggests that 7 wt. % of Ce and 5 wt. % of Ni are considerably enhancing the formation of active sites and catalyst structural properties, which exhibited the highest catalytic performance. Moreover, enhancement performance of NCS7 was suggested due to the high Ni dispersion on the SBA-15 surfaces as evidenced by XRD and TEM. The substitution of the Ni and Ce species to the surface silanol groups was evidenced by FTIR analysis. The

stability of catalyst could be increased by addition of Ce species, in which the Ce species can prevent the carbon deposition at high reaction temperature of 700°C. Sun *et al* observed when the rare earth metal oxide CeO_2 was added, the generation of surface oxygen species could be enhanced and led to mitigation of carbon deposition.[16] The increasing of Ce loading over the composite catalyst could enhance basic strength of catalyst, leading to promote the CO_2 adsorption, improve the activity and inhibit carbon deposition.[17] The poor catalytic performance of NCS1 was suggested due to the less active site of Ce species on the catalyst surfaces.

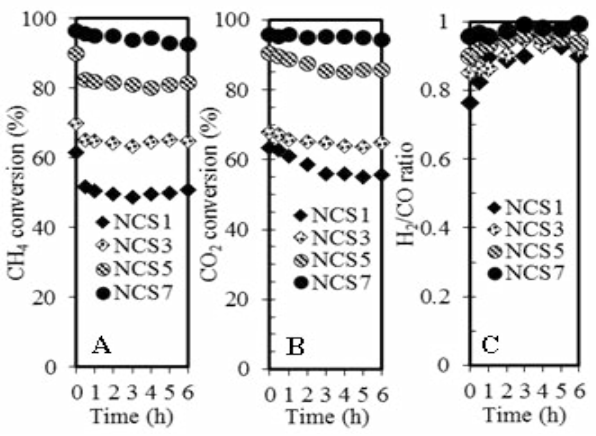

Figure 4. CO_2 reforming of methane over NCS1, NCS3, NCS5 and NCS7 catalyst, (A) CH4 conversion, (B) CO_2 conversion and (C) H_2/CO ratio.

4. Conclusion

All of NCS catalysts prepared by sol-gel method were well preserved the meso-porous structure of SBA-15 with high surface area (670.69 $m^2 g^{-1}$). NCS7 showed the high catalytic activity with CH_4 conversion, CO_2 conversion and H_2/CO ratio of 94.9%, 95.1%, and 0.99, respectively. The addition of Ce result in an enhancement of the Ni dispersion could create a suitable active site for reaction. All catalyst showed a good stability correlated to the properties of SBA-15 and significant role of Ce to prevent the carbon formation.

5. Acknowledgements

The authors gratefully acknowledge the financial support from RDU140391 and RDU140398 granted by Universiti Malaysia Pahang and RDU150126 granted by Ministry of Higher Education, Malaysia.

6. References

1. Yan BH, Wang Q, Jin Y, Cheng Y. Dry reforming of methane with carbon dioxide using pulsed DC arc plasma at atmospheric pressure. Plasma Chemistry and Plasma Processing. 2010 Apr 1; 30(2):257–66. Crossref
2. Craciun R, Daniell W, Knözinger H. The effect of CeO_2 structure on the activity of supported Pd catalysts used for methane steam reforming. Applied Catalysis A: General. 2002 Apr 30; 230(1):153–68. Crossref
3. Pompeo F, Nichio NN, Souza MM, Cesar DV, Ferretti OA, Schmal M. Study of Ni and Pt catalysts supported on α-Al2O3 and ZrO2 applied in methane reforming with CO_2. Applied Catalysis A: General. 2007 Jan 10; 316(2):175–83. Crossref
4. Fan MS, Abdullah AZ, Bhatia S. Catalytic technology for carbon dioxide reforming of methane to synthesis gas. Chem Cat Chem. 2009 Oct 5; 1(2):192–208. Crossref
5. Zhang S, Muratsugu S, Ishiguro N, Tada M. Ceria-doped Ni/SBA-16 catalysts for dry reforming of methane. ACS Catalysis. 2013 Jul 22; 3(8):1855–64. Crossref
6. Albarazi A, Beaunier P, Da Costa P. Hydrogen and syngas production by methane dry reforming on SBA-15 supported nickel catalysts: on the effect of promotion by Ce 0.75 Zr 0.25 O_2 mixed oxide. International Journal of Hydrogen Energy. 2013 Jan 11; 38(1):127–39. Crossref
7. Laskowski Ł, Laskowska M, Bałanda M, Fitta M, Kwiatkowska J, Dziliński K, Karczmarska A. Mesoporous silica SBA-15 functionalized by nickel–phosphonic units: Raman and magnetic analysis. Microporous and Mesoporous Materials. 2014 Dec 31; 200:253–9. Crossref
8. Aziz MA, Jalil AA, Triwahyono S, Saad MW. CO_2 methanation over Ni-promoted mesostructured silica nanoparticles: Influence of Ni loading and water vapor on activity and response surface methodology studies. Chemical Engineering Journal. 2015 Jan 15; 260:757–64. Crossref
9. Yan H, Lu P, Pan Z, Wang X, Zhang Q, Li L. Ce/SBA-15 as a heterogeneous ozonation catalyst for efficient mineralization of dimethyl phthalate. Journal of Molecular Catalysis A: Chemical. 2013 Oct 31; 377:57–64. Crossref
10. Thitsartarn W, Maneerung T, Kawi S. Highly active and durable Ca-doped Ce-SBA-15 catalyst for biodiesel production. Energy. 2015 Sep 30; 89:946–56. Crossref
11. Mahoney EG, Pusel JM, Stagg-Williams SM, Faraji S. The effects of Pt addition to supported Ni catalysts on dry (CO_2) reforming of methane to syngas. Journal of CO2 Utilization. 2014 Jun 30; 6:40–4.
12. Quek XY, Liu D, Cheo WN, Wang H, Chen Y, Yang Y. Nickel-grafted TUD-1 mesoporous catalysts for carbon dioxide reforming of methane. Applied Catalysis B: Environmental. 2010 Apr 6; 95(3):374–82. Crossref

13. Ma Z, Wang X, Wei S, Yang H, Zhang F, Wang P, Xie M, Ma J. Cu (I) immobilized on functionalized SBA-15: A recyclable catalyst for the synthesis of 1, 3-diynes using terminal alkynes without base. Catalysis Communications. 2013 Sep 5; 39:24–9. Crossref
14. Ye W, Lin Z, Dong B, Kang J, Zheng X, Wang X. Preparation and Catalytic Properties of Ti-SBA-15 Mesoporous Materials. Materials Sciences and Applications. 2011 Jun 24; 2(06):661. Crossref
15. Alipour Z, Rezaei M, Meshkani F. Effects of support modifiers on the catalytic performance of Ni/Al_2O_3 catalyst in CO_2 reforming of methane. Fuel. 2014 Aug 1; 129:197–203. Crossref
16. Feng-man Sun, Chang-feng Yan, Zhi-da Wang, Chang-qing Guo, Shi-lin Huang. Ni/CeeZreO catalyst for high CO_2 conversion during reverse water gas shift reaction (RWGS). International journal of hydrogen energy. 2015; 40:15985–93. Crossref
17. Mingchen T, Long X, Maohong F. Effect of Ce on 5 wt% Ni/ZSM-5 catalysts in the CO_2 reforming of CH_4 reaction. International journal of hydrogen energy. 2014 Aug 21; 39:15482–96. Crossref